Indices of Violent Tornado Environments

ARIEL E. COHEN
National Weather Service, Jackson, Mississippi

(Manuscript received 7 July 2010; in final form 14 November 2010)

ABSTRACT

Despite their rarity, the extreme impacts of violent tornadoes require that forecasters be able to identify meteorological ingredients and spatial patterns of key meteorological variables associated with past violent tornadoes. Using Rapid Update Cycle-2 analyses from the Storm Prediction Center, this study identifies some of the commonalities among mesoscale parameters associated with 46 violent tornadoes that occurred between 2003 and 2010. The commonalities include high values of 0-1 km and 0-3 km storm-relative helicity (SRH) and 0-1 bulk shear magnitude, as well as moderate amounts of surface-based and mixed-layer convective available potential energy. The violent tornadoes were often found to occur on the northern spatial gradient of the significant tornado parameter. High ratios of 0-1 km SRH to 0-3 km SRH were also determined to characterize the near-storm environments around the violent tornadoes. This work is intended to provide forecasters with guidance in identifying environments supportive of violent tornadoes, and potentially in mentioning violent tornadoes in outlooks, forecasts, and discussions.

1. Introduction

On 24 April 2010, a deadly, long-track tornado traveled from northeastern Louisiana across portions of central Mississippi, causing EF-4 damage with maximum estimated winds of 170 mph (76 m s^{-1}) in Yazoo City, Mississippi and further east into Holmes County. Ten deaths and over one hundred injuries occurred from this tornado. This tornado was one of many during a two-day severe weather event, which was characterized by high values of low-level and deep-layer vertical wind shear and moderate instability. This combination resulted in extreme values of several mesoscale indices, including the significant tornado parameter (STP) and the supercell composite parameter (SCP). In evaluating the tornadic potential prior to the event, forecasters noted these values and speculated on how intense any tornadoes might become. Although the potential for strong tornadoes was fairly certain, the potential for violent tornadoes was not as

Corresponding Author Address: Ariel Cohen, National Weather Service, Jackson, Mississippi
234 Weather Service Drive, Flowood, MS 39232
E-Mail: Ariel.Cohen@noaa.gov

clear. This event provided the impetus to explore the potential for environments to support violent tornadoes.

The Yazoo City tornado was indeed a rare event. However, on occasion, forecasters face the extreme-impact forecast challenge of assessing the potential for significant tornadoes, which can be accomplished by studying environments associated with violent tornadoes of the past. Thompson et al. (2003, hereafter T03), and Thompson et al. (2004, hereafter T04), provided a substantial amount of parameter analysis for discriminating among near-storm environments (NSEs) supporting significantly tornadic supercells (EF-2 or greater tornado damage), weakly tornadic supercells (EF-0 or EF-1 tornado damage), and nontornadic supercells. They studied 413 proximity soundings for these supercells derived from hourly analyses based on the Rapid Update Cycle-2 (RUC-2) model. Similarly, Davies (2004) examined RUC model proximity soundings for a large sample of tornadic and nontornadic supercells, while other prior studies focused on broader proximity criteria with observed soundings (e.g., Rasmussen and Blanchard, 1998; Craven and Brooks, 2004).

T03 and T04 implied an ingredients-based approach to evaluate the maximum intensity of tornadoes with supercells that a mesoscale environment could support. The ingredients focus on quantities directly calculated from forecast soundings [including variations of convective available potential energy (CAPE) and convective inhibition (CIN), low-level and deep-layer bulk wind difference, storm-relative helicity (SRH), and lifted condensation level (LCL)]. They developed guidance including the STP and the SCP, both of which represent nonlinear combinations of the aforementioned ingredients. T03 presented the original analyses of these composite parameters, which were then updated in T04 as follows:

$$\text{SCP} = (\text{most-unstable CAPE} / 1000\ \text{J kg}^{-1}) * (\text{effective bulk wind difference} / 20\ \text{m s}^{-1}) * (\text{effective SRH} / 50\ \text{m}^2\ \text{s}^{-2})$$

$$\text{STP} = (\text{mixed-layer CAPE} / 1500\ \text{J kg}^{-1}) * (\text{effective bulk wind difference} / 20\ \text{m s}^{-1}) * (\text{effective SRH} / 150\ \text{m}^2\ \text{s}^{-2}) * ((2000 - \text{mixed-layer LCL}) / 1500\ \text{m}) * ((250 + \text{mixed-layer CIN}) / 200\ \text{J kg}^{-1})$$

The effective bulk wind difference term in these formulae is capped at a value of 30 m s^{-1}, and the MLCIN term is set to one once MLCIN exceeds -50 J kg^{-1}.

Using the 54 proximity soundings for significant tornado cases that T03 documented, statistical analyses for several variables were presented in T03, T04, and Thompson et al. (2007, hereafter T07). Figure 1 displays selected portions of figures provided in these studies. Additionally, T07 defined the effective SRH (ESRH) and illustrated its ability to discriminate between NSEs associated with significantly tornadic supercells and nontornadic supercells. ESRH is computed throughout the effective inflow layer depth, which is defined as the layer of the atmosphere through which the amount of CAPE and CIN generated by lifting a parcel from each level within the layer exceed certain constraints. The ESRH results in T07 are presented for CAPE and CIN using constraints of 100 J kg^{-1} and -250 J kg^{-1} (also reproduced in Fig. 1). All storm-relative parameters presented herein assume storm motion for a right-moving supercell, with any predicted motion using techniques derived from Bunkers et al. (2000).

Even rarer than facing the forecast challenge of assessing environments capable of producing strong tornadoes (EF-2 or EF-3) is the challenge of forecasting violent tornadoes (EF-4 or EF-5). Little, if any, guidance exists for the distribution of parameters that characterize the NSEs solely around violent tornadoes (primarily due to small sample sizes). While it could be inferred that using the upper echelons of the parameter space for significant tornadoes shown in

T03, T04, and T07 could aid forecasters in assessing violent tornado potential, this is not necessarily the case, since the significant tornado sample is heavily dominated by relatively "weaker" tornadoes. Naturally, violent tornadoes only account for a very small proportion of reported tornadoes, and violent damage is representative of only a fraction of the total tornado damage path. In fact, upon querying the official tornado reports provided by the *SeverePlot* program (Hart and Janish, 2006), only 5.2% of significant tornadoes and 1.1% of all tornadoes between 1 January 1950 and 31 December 2009 were violent tornadoes in the United States. Despite their rarity, they provide very high impact to the American public, having been responsible for 3,296 deaths, 43,057 injures, and $3.96 billion of damage, which highlights the need to recognize their environments. Thus, the purpose of the present work is to provide an analysis of NSE variables that are shared among violent tornado cases. T03, T04, and T07 all provide the motivation for the variables analyzed in the present study.

2. Data collection and methodology

The present study identifies 46 violent tornadoes that occurred across the continental United States between 2003 and 2010. Several different parameters describing the NSE of each violent tornado were collected by comparing the location of each violent tornado with RUC-2 analysis output (using 40-km grid spacing) provided by the Storm Prediction Center (2010) within one hour of the violent tornado. These data are provided for numerous mesoscale parameters and were used to characterize the NSE around each violent tornado. They were automatically extracted for each of the cases from 2003 to 2009. Note that during this period, the grid-spacing of the RUC-2 changed from 20 km to 13 km in June 2005. For the 2010 cases, these archives were used to manually evaluate the parameters, which involved rough

interpolations between parameter contours on their plan views of the RUC-2 output. While this manual process introduces some error, forecasters regularly evaluate plan views of these parameters on a real-time basis in a subjective fashion, and thus this was the technique employed in the present study.

After the parameter data were extracted, a scatter plot of each parameter was generated showing the entire distribution of values. The current study presents each of these scatter plots and is intended to improve our understanding of the environments that have supported violent tornadoes. This information is most applicable in a real-time or nowcasting mode given its derivation from RUC-2 analysis output. However, its utility could be extended toward somewhat longer term forecasts if confidence in particular ingredients increases based on ensemble consensus (e.g., when the majority of members of the Short-Range Ensemble Forecast System yield a particular parameter threshold). Thus, the results of this study could provide guidance to forecasters in mentioning violent tornadoes in forecasts and outlooks.

It must also be noted that there is considerable uncertainty in the classification of a violent tornado. For example, tornadoes that occur in the open countryside are less likely to damage structures causing a more difficult estimation of tornado intensity (Doswell and Burgess, 1988). On the other hand, Schaefer and Galway (1982) found that tornadoes affecting more populated areas have higher ratings than those in open country based on the tornado climatology in the western plains from Oklahoma to the Dakotas. These studies, along with Kelly et al. (1978) and Grazulis (1993), note that discrepancies in tornado intensities in the tornado climatology can be attributed to population biases and heterogeneous distributions of structures. In addition to these factors, there is ultimately uncertainty in classifications across boundaries in the EF-scale, which further adds uncertainty to the more marginal ratings. Nevertheless, there is

confidence that the dataset of violent tornadoes from 2003 to 2010 is sufficiently robust to reduce error contributed by tornado rating uncertainty.

3. Analysis

To aid forecasters in recognizing spatial patterns of STP occurring in association with violent tornadoes, Fig. 2 provides the approximate positions of 20 selected violent tornadoes overlaid on plan views of STP including mixed-layer CIN occurring within one hour of the tornadoes. For comparison to strong tornadoes, a similar analysis is done in Fig. 3 as in Fig. 2, except for 20 selected strong tornado cases in Fig. 3. It is immediately apparent from these figures that most of the significant tornadoes rarely occur within the maximum of STP and are usually found on the spatial gradient.

To quantify this phenomenon, each of the 40 cases was further classified according to where the tornado occurred within to the spatial gradient relative to the maximum STP. To do this, the position of each tornado was compared to the orientation of the STP contours, and a subjective classification was made on its position relative to the spatial gradient. Table 1 specifies the proportion of violent and strong tornado reports occurring in each of the classified areas. The majority of significant tornado reports occurred within the northern gradient, and this is likely where low-level shear is maximized in the presence of relatively weaker instability (e.g., along a warm front, as opposed to deep within the warm sector). Having almost no significant tornadoes occurring in the southern gradient is likely a reflection of the larger quantities of convective inhibition in the absence of stronger forcing. The analysis of low-level boundaries and the large-scale pattern linked to the boundaries, can also play a critical role in pattern recognition for assessing the potential for violent tornadoes.

In spite of the similarities in the spatial pattern of the violent and strong tornadoes relative to the spatial distribution of STP, especially in regards to the occurrence of tornadoes on spatial gradients, the areawide maxima in STP are noticeably different between the violent and strong tornado cases. In particular, the areawide maxima appear lower in the strong tornado cases than in the violent tornado cases. This is illustrated in Fig. 4, which presents the distributions of the areawide maxima in STP to provide characteristic values of STP that are most likely to stand out to meteorologists when viewing a plan view of STP.

Figure 5 provides the first in the series of scatter plots specifying each of the parameter values describing the NSE of each violent tornado, along with the 25^{th}, 50^{th}, and 75^{th} percentile and mean values overlaid on each plot. For STP, the interquartile range (25^{th} to 75^{th} percentile) for violent tornadoes is at the upper end of the distribution of STP identified in T04, though overlap is noted. This overlap suggests that an exceptionally high value of STP is not a prerequisite for violent tornadoes, which is consistent with findings from Thompson et al. (2010). While increasing values of the aforementioned parameters do require substantial attention, they do not alone indicate violent tornado NSEs. This finding reflects that revealed from Fig. 2: violent tornadoes do not commonly occur in the maxima of the composite parameters, but rather on the gradients.

Figure 6 suggests that, while there is a rough threshold of around 750 J kg^{-1} of MLCAPE and SBCAPE needed for violent tornado NSEs, high to extreme values of CAPE are not necessary. This does not preclude the presence of higher values of CAPE elsewhere across a larger area, as implied by Fig. 2; rather it may merely be another reflection of the violent tornadoes occurring on the spatial gradients of derived parameters. Given the similarity in the distributions of low-level parcel buoyancy for the violent tornado NSEs and those of significant

tornadoes investigated in T03, it is speculated that there must be compensating factors that distinguish violent tornado NSEs from the remainder of the significant tornado distribution.

One compensating factor is evident in Fig. 7: the interquartile ranges for 0-1 km SRH and ESRH are around 200 $m^2 s^{-2}$ greater than those identified in T03. These results present one key distinguishing factor between violent tornado environments and the aggregated significant tornado environments – the magnitudes of low-level shear found in violent tornado environment are at the upper end of the distribution of significant tornado environments. It is likely the case that directional shear plays a significant role in generating such high values of low-level SRH in violent tornado NSEs. With at least marginal amounts of instability for deep convection noted in Fig. 6, the strong horizontal vorticity is tilted into the vertical and stretched, possibly providing a key impetus for violent tornadogenesis.

Figure 7 indicates very small differences between the 0-1 km and 0-3 km SRH data. To further investigate this finding, a ratio of 0-1 km to 0-3 km SRH was computed for each of the 46 violent tornado NSEs, as seen in Fig. 8. This figure indicates that ratios for most of the cases experienced were generally at least 75%. This suggests that the majority of low-level SRH is contained within the 0-1 km layer, or closest to the ground. This finding partially confirms some of the research provided by Esterheld and Guiliano (2008), who found that significant tornado NSEs were characterized by an angle between the storm-relative inflow vector and 10-500-m shear vector around 90 degrees, with a long, straight-line hodograph in the surface-to-500-m layer. Figure 9 provides evidence for the extreme values of low-level shear (0-1 km layer), which are well above those determined in T04. Such environments imply large quantities of streamwise vorticity within the boundary layer, which can be ingested into updrafts to support tornadogenesis. Similar findings were revealed by Markowski et al. (2003a), who studied 400

vertical wind profiles associated with tornadic and nontornadic supercells obtained from RUC-2 output. Consistent with the present study, they found environments characterizing significantly tornadic supercells to be characterized by substantially larger low-level vertical wind shear, streamwise vorticity, and SRH relative to those environments characterizing nontornadic and weakly tornadic supercells.

Magnitudes of 0-8 km bulk shear were also investigated in the present work. This parameter was found to be useful in discriminating between environments associated with long-track tornadoes and short-track tornadoes in Garner (2007). Garner (2007) found the interquartile range of 0-8 km bulk shear magnitudes for long-track tornadoes to be nearly identical to that found for violent tornadoes in the present study, as seen in Fig. 10. This suggests that violent tornadoes are also associated with the quantities of deep-layer shear associated with long-track tornadoes (versus short-track tornadoes). This finding is important, because tornadoes that travel greater distances are more likely to produce greater amounts of damage compared to short-track tornadoes, and the potential for long-track tornadoes could be elevated in similar environments as violent tornadoes.

In addition to associating long-track tornadoes with larger magnitudes of 0-8 km bulk shear, Garner (2007) also investigated the relationship between tornado path length and surface temperature-dewpoint depression and found smaller depressions to characterize the environments of long-track tornadoes. Smaller depressions have been found to favor a more positively buoyant rear flank downdraft (Markowski et al., 2003b), thus potentially promoting greater tornado longevity and a greater chance for the tornado to produce damage. As a proxy for temperature-dewpoint depressions, mean layer lifting condensation level (MLLCL) height is explored in the present study, which is physically positively correlated with the temperature-

dewpoint depressions (i.e., greater low-level moisture is associated with lower MLLCL heights). These values are around 100 m lower than those presented in T03, suggesting greater quantities of low-level moisture in the violent tornado NSEs, as seen in Fig. 10.

4. Conclusions

This study identified commonalities in the near-storm environments (NSEs) among 46 violent tornado cases. The violent tornadoes were found to occur at the northern spatial gradient of STP in around half of a subset of the cases, as opposed to only around a quarter near the spatial maxima of this parameter. This highlights the need to carefully analyze the synoptic-scale pattern and presence of low-level boundaries, as these gradients are often coincident with boundaries, which are often tied to the large-scale pattern.

Scatter plots were also evaluated for several different parameters obtained from RUC-2 analysis fields. High values of low-level shear and SRH were found to exist in these NSEs, with moderate amounts of SBCAPE and MLCAPE, though possibly less CAPE than that which characterizes the broader distribution of significant tornadoes. The amount of SRH in the 0-1-km layer was found to comprise the majority of the SRH in the 0-3-km layer. Large magnitudes of 0-8 km bulk shear and low LCL heights characterize the environments of violent tornadoes, as they do in discriminating long-track from short-track tornadoes.

This work provides preliminary guidance to characterizing mesoscale environments supportive of violent tornadoes and provides general ranges of values observed for NSEs supporting violent tornadoes. Forecasters could also use this work as guidance prior to mentioning violent tornadoes in outlooks, forecasts, and discussions, but are also cautioned of the small sample size and considerable overlap in the distributions.

Acknowledgements. I thank the staff of the National Weather Service in Jackson, Mississippi, particularly Mr. Alan Gerard and Mr. Greg Garrett for their inspiration in developing forecasting tools for violent tornadoes, as well as their reviews of this work. Special thanks also go to Matthew Bunkers (National Weather Service, Rapid City, SD) and Richard Thompson (Storm Prediction Center) for their thorough and insightful reviews of this work. I am very grateful for the RUC-2 output that Mr. Thompson provided, which greatly expanded the sample size studied in this work. Additionally I also thank Laura Kanofsky (National Weather Service St. Louis, Missouri) for reviews of this work, along with all editors for their input in bettering this work. All of their feedback greatly improved the quality of this work.

REFERENCES

Bunkers, M. J., B. A. Klimowski, J. W. Zeitler, R. L. Thompson, and M. L. Weisman, 2000: Predicting supercell motion using a new hodograph technique. *Wea. Forecasting*, **15**, 61–79.

Craven, J. P., and H. E. Brooks, 2004: Baseline climatology of sounding derived parameters associated with deep, moist convection. *Natl. Wea. Dig.*, **28**, 13–24.

Davies, J. M., 2004: Estimations of CIN and LFC associated with tornadic and nontornadic supercells. *Wea. Forecasting*, **19**, 714-726.

Doswell, C. A., III, and D. W. Burgess, 1988: Some issues of United States tornado climatology. *Mon. Wea. Rev.*, **116**, 495-501.

Esterheld, J. M. and D. J. Guiliano, 2008: Discriminating between tornadic and nontornadic supercells: A new hodograph technique. *Electronic Journal of Severe Storms Meteorology*, **3 (2)**, 1–50.

Garner, J., 2007: A preliminary study on environmental parameters related to tornado path length. *National Weather Association Electronic Journal of Operational Meteorology*, 2007-EJ5. (http://www.nwas.org/ej/2007-EJ5/)

Grazulis, T. P., 1993: A 100-Year Perspective of Significant Tornadoes. The Tornado: Its Structure, Dynamics, Prediction, and Hazards. *Geophys. Monogr.* **79**, 467-474.

Hart, J. A., and P. R. Janish, cited 2006: SeverePlot: Historical severe weather report database. Version 2.0. Storm Prediction Center, Norman, OK. (http://www.spc.noaa.gov/software/svrplot2/)

Kelly, D. L., J. T. Schaefer, R. P. McNulty, C. A. Doswell III, and R. F. Abbey, Jr., 1978: An augmented tornado climatology. *Mon. Wea. Rev.*, **106**, 1172-1183.

Markowski, P. M., C. Hannon, J. Frame, E. Lancaster, A. Pietrycha, R. Edwards and R.L. Thompson, 2003a: Characteristics of vertical wind profiles near supercells obtained from the Rapid Update Cycle. *Wea. Forecasting*, **18**, 1262-1272.

_____, P. M., J. M. Straka, and E. N. Rasmussen, 2003b: Tornadogenesis resulting from the transport of circulation by a downdraft: Idealized numerical simulations. *J. Atmos. Sci.*, **60**, 795-823.

Rasmussen, E. N., and D. O. Blanchard, 1998: A baseline climatology of sounding-derived supercell and tornado parameters. *Wea. Forecasting*, **13**, 1148-1164.

Thompson, R. L., R. Edwards, J. A. Hart, K. L. Elmore, and P. M. Markowski, 2003: Close proximity soundings within supercell environments obtained from the Rapid Update Cycle. *Wea. Forecasting*, **18**, 1243–1261.

_____, _____, and C. Mead, 2004: An update to the supercell composite and significant tornado parameters, Preprints, *22nd Conf. of Severe Local Storms*, Hyannis, MA, CD-ROM, P8.1.

_____, _____, _____, 2007: Effective storm-relative helicity and bulk shear in supercell thunderstorm environments. *Wea. Forecasting*, **22**, 102-115.

_____, B. T. Smith, J. S. Grams, A. R. Dean, and C. Broyles, 2010: Climatology of near-storm environments with convective modes for significant severe thunderstorms in the contiguous United States, Preprints, *25th Conf. on Severe Local Storms*, Denver, CO, Amer. Meteor. Soc., 16B.6.

Schaefer, J. T., and J. G. Galway, 1982: Population biases in the tornado climatology, Preprints, *12th Conf. On Severe Local Storms*, San Antonio, TX, Amer. Meteor. Soc., 51-54.

Storm Prediction Center cited 2010: SPC Hourly Mesoscale Analysis. (http://www.spc.noaa.gov/exper/ma_archive)

TABLES AND FIGURES

Table 1. Distribution of significant tornadoes relative to the spatial gradient of the Significant Tornado Parameter. "NW" denotes "northwestern gradient," "N" denotes "northern gradient," "NE" denotes "northeastern gradient," "W" denotes "western gradient," "MAX" denotes spatial maximum, "SE" denotes "southeastern gradient," "S" denotes "southern gradient," and "SW" denotes "southwestern gradient."

Geographic Area	**Percent of EF4 or EF5 tornadoes Occurring in the Specified Geographic Area**	**Percent of EF2 or EF3 tornadoes Occurring in the Specified Geographic Area**
NW/N/NE	50%	55%
W/E	20%	30%
MAX	30%	10%
SE/S/SW	0%	5%

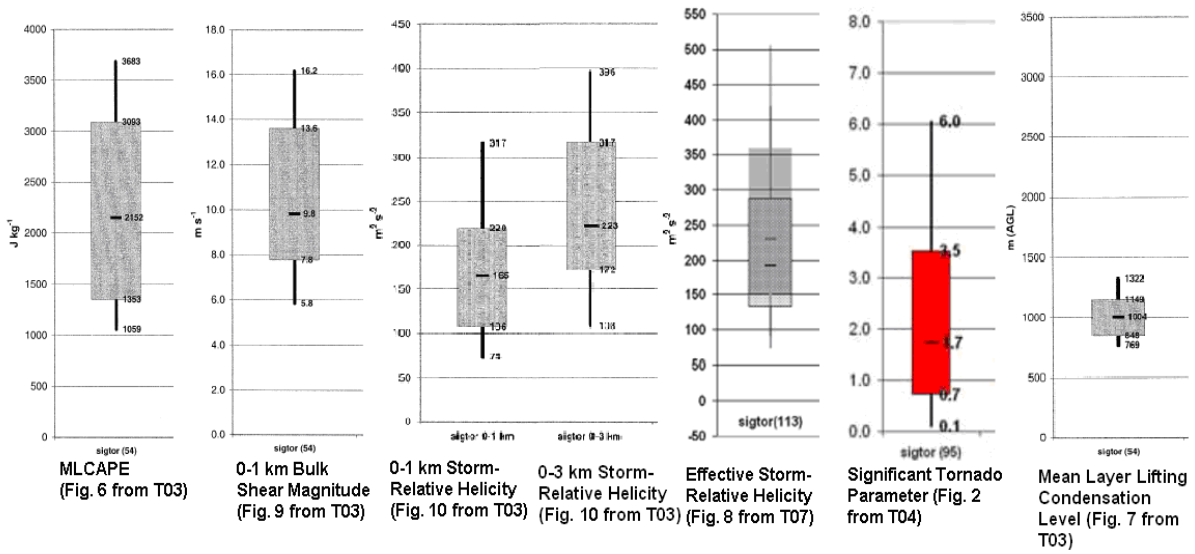

Figure 1. Selected portions of several figures from T03, T04, and T07 illustrating results for significant tornadoes.

Figure 2. Regional distribution of violent tornadoes (black dot), STP (contours), and mixed-layer CAPE (light blue and dark blue shading indicates between 25 and 50 J kg^{-1} and over 50 J kg^{-1} of mixed-layer CIN, respectively). Annotations specify the position of the point relative to the spatial gradient of STP using the nomenclature specified in Table 1.

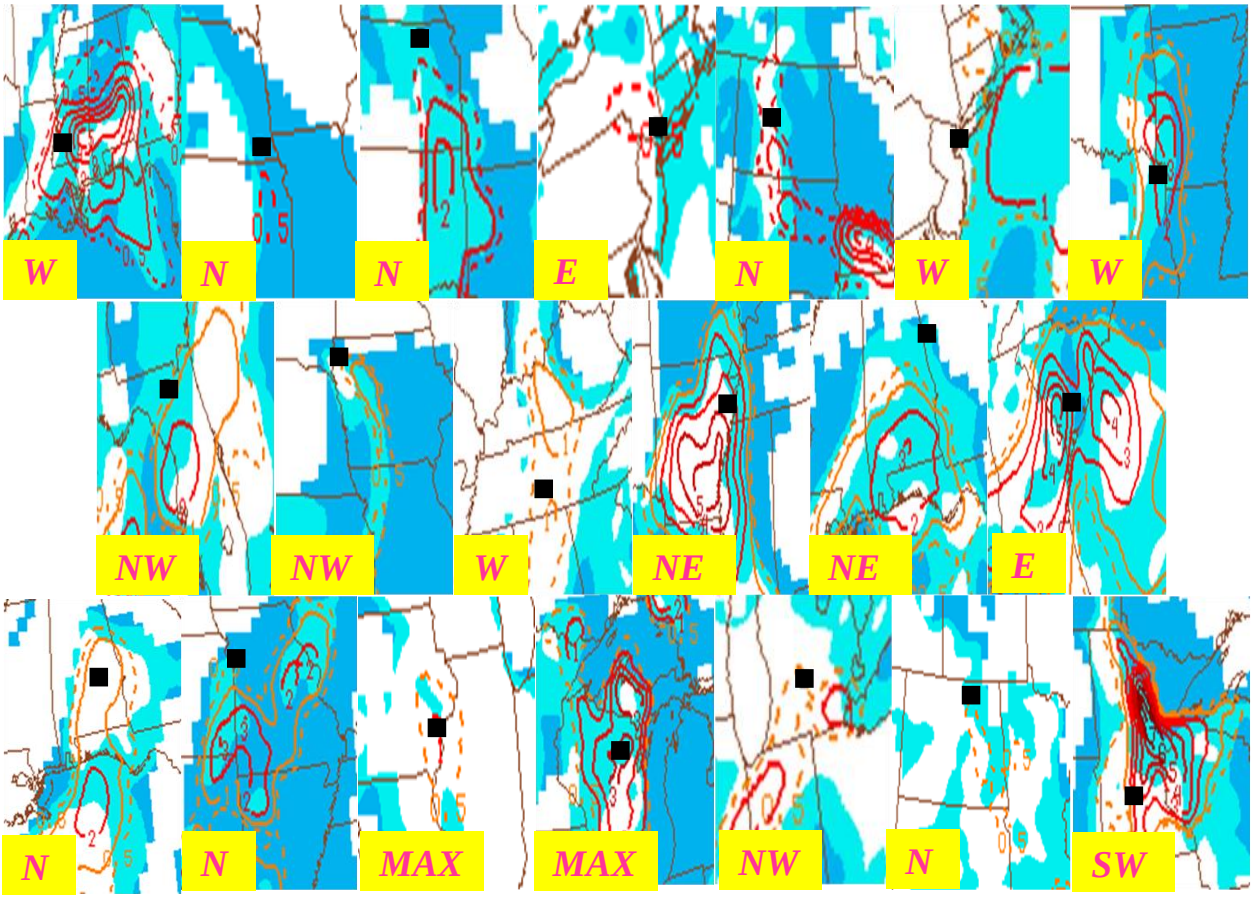

Figure 3. Same as Fig. 2 except for strong tornadoes.

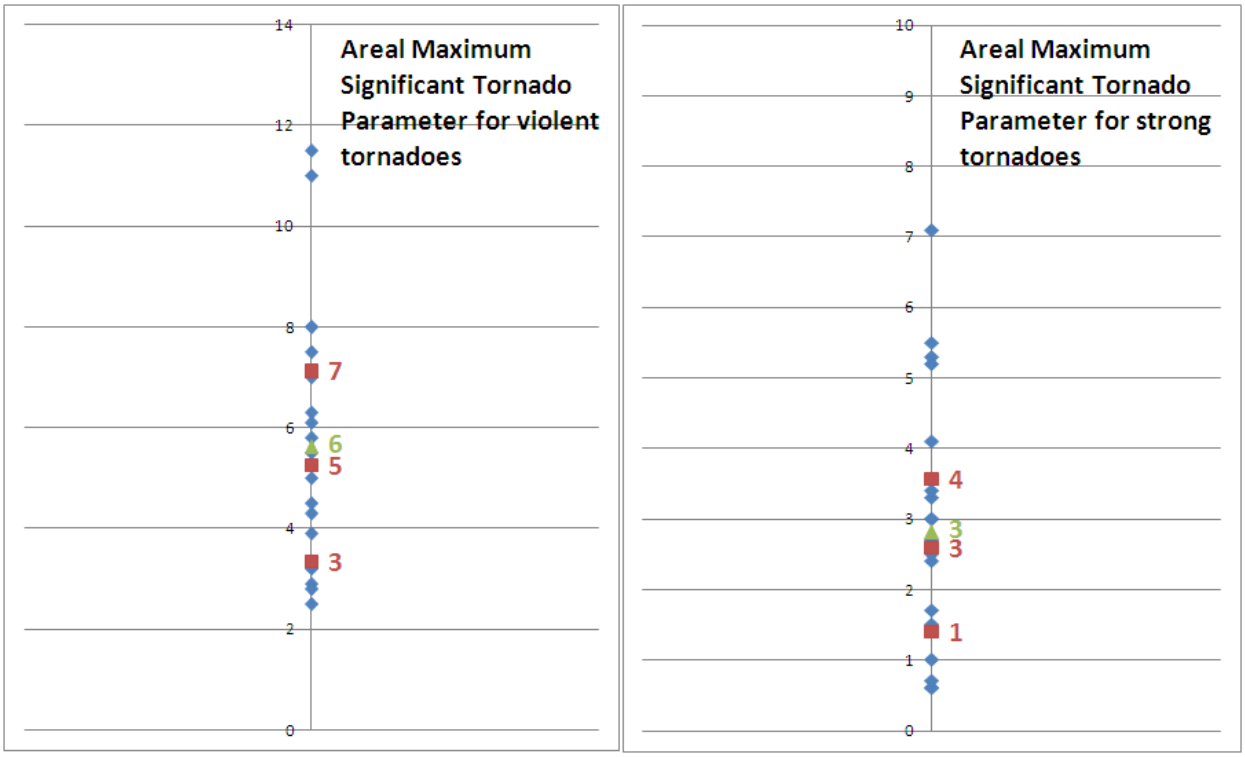

Figure 4. Distribution of the areal maximum STP values among violent and strong tornado cases, as well as the 25th percentile (lower red square), 50th percentile (middle red square), 75th percentile (upper red square), and mean (green triangle) of each distribution.

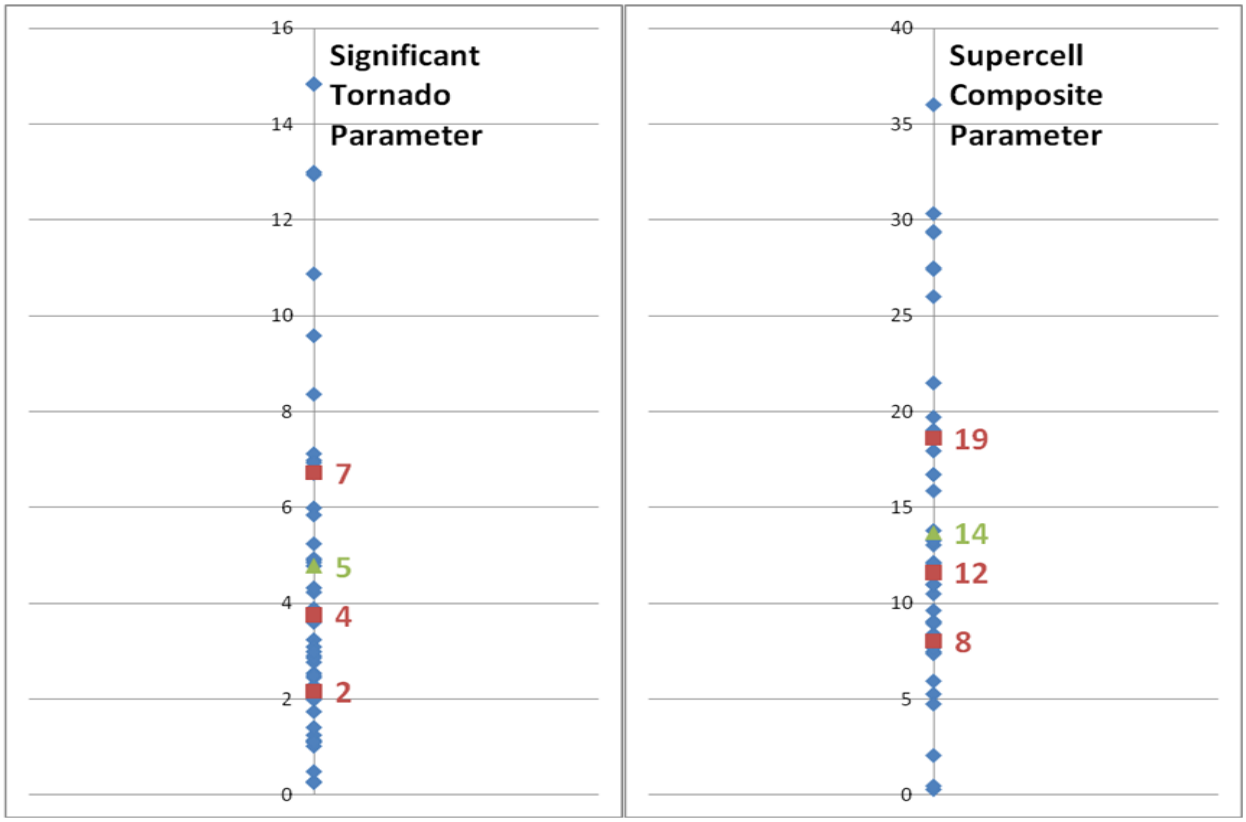

Figure 5. Same as Fig. 4 except for strong tornadoes.

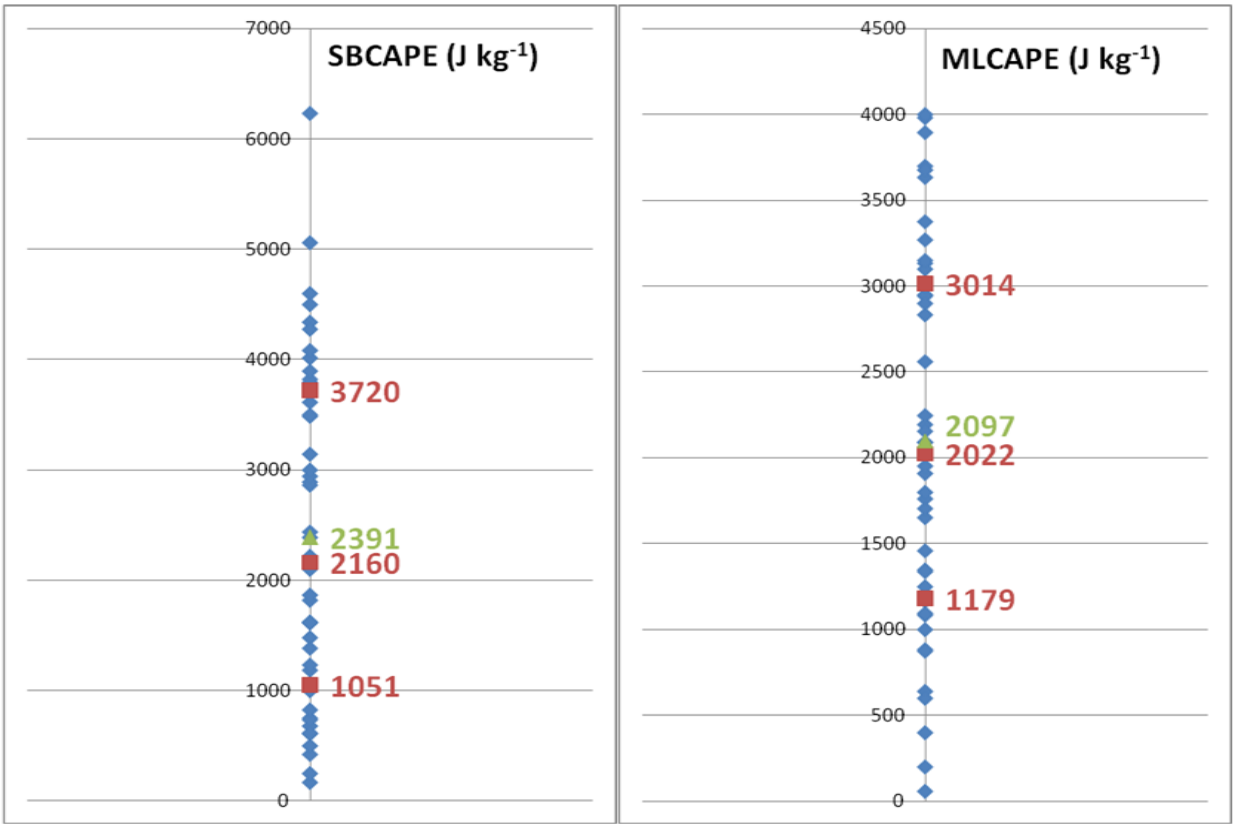

Figure 6. Distribution of SBCAPE and MLCAPE in the NSEs among violent tornado cases, as well as the 25th percentile (lower red square), 50th percentile (middle red square), 75th percentile (upper red square), and mean (green triangle) of each distribution.

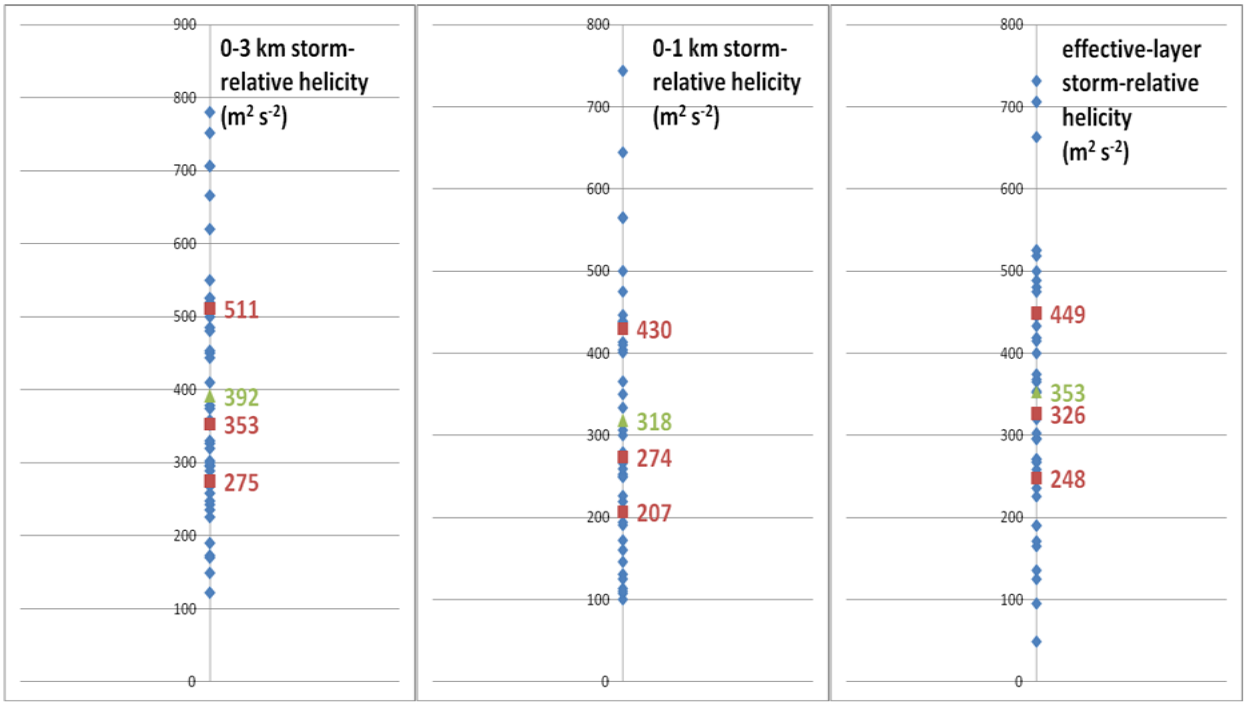

Figure 7. Same as Fig. 6 except for 0-3 km SRH, 0-1 km SRH, and ESRH.

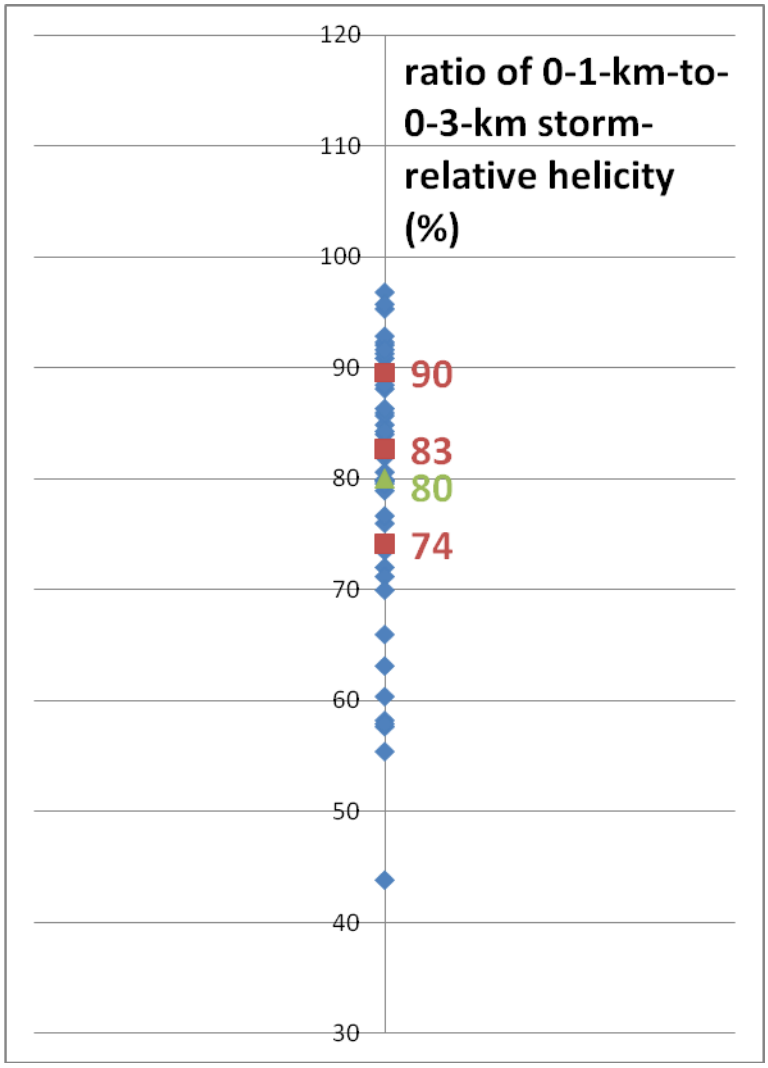

Figure 8. Same as Fig. 6 except for ratio of 0-1 km SRH to 0-3 km SRH.

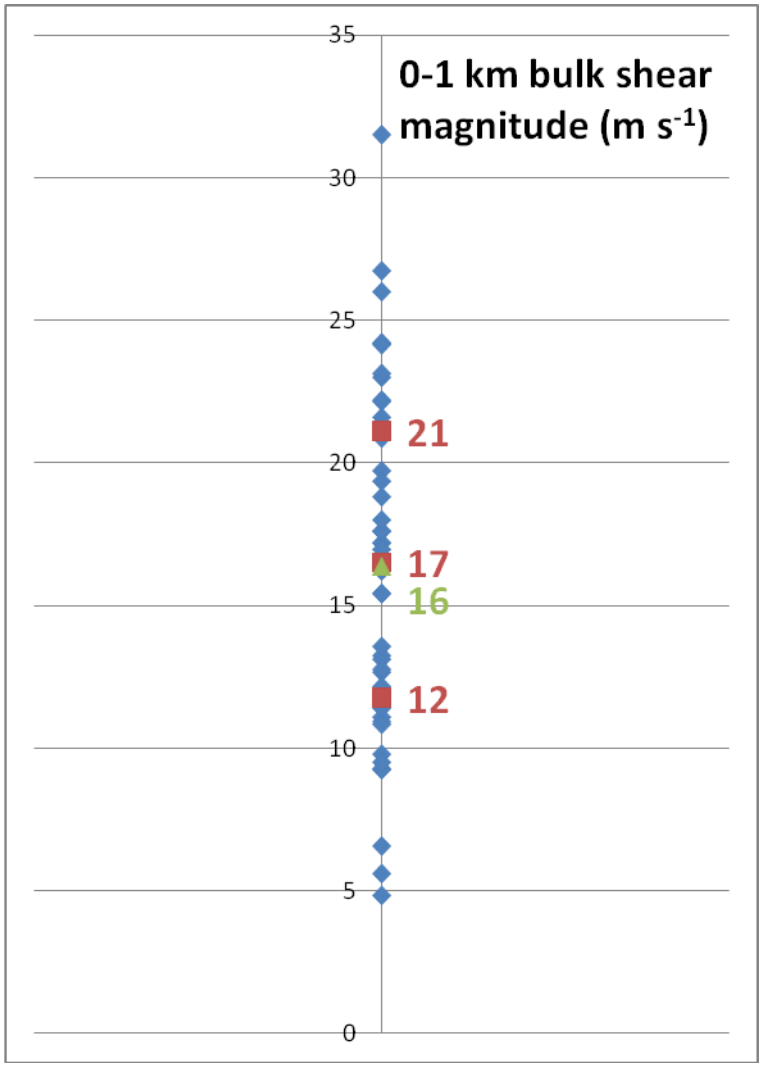

Figure 9. Same as Fig. 6 except for 0-1 km bulk shear.

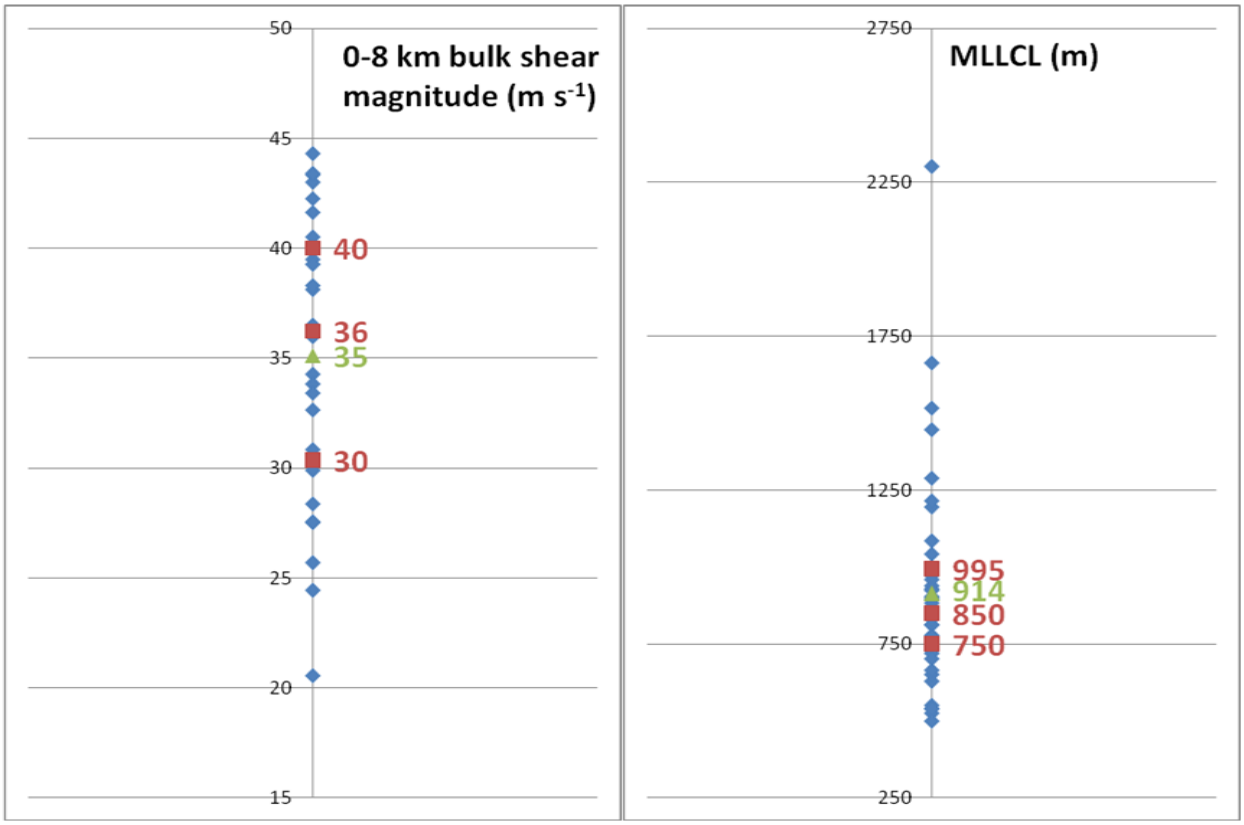

Figure 10. Same as Fig. 6 except for 0-8 km bulk shear magnitude and MLLCL height.